AB-10-XXX
ASHRAE2010-85028 Track 12 Unassigned Session: 12-1 Clean Rooms

# Understanding of flow and scalar fields by combining Measured Data and CFD

**Akira Kondo, PhD** **Hiroshi Nakagawa** **Akikazu Kaga, PhD** **Yoshio Inoue, PhD**

*ABSTRACT*

*A cost function expressed by the remainders of the governing equations and the difference between observed values and the solutions was proposed. This method was applied for a two-dimensional room and the performances of the cost function method were examined. The individual type solution, which the governing equation of a variable is partially differentiated with respect to itself, and the integrated type solution, which the governing equation of a variable is partially differentiated with respect to another variable, were compared. The performances of the integrated type solution for combining three data of temperature, concentration and wind components gave the excellent results for all variables than that of the individual type solution.*

## INTRODUCTION

In fluid dynamic engineering, it is important to understand both flow and scalar fields in a target region. Measurements or Computational fluid dynamics (CFD) are usually used for understanding flow and scalar fields except for simple fields which can be analytically solved and these two techniques had been independently developed(Leonard 1974; Rodi 1976; Launder 1975; Kaga 1993). Since CFD has inevitably errors accompanied by discretization and numerical calculation, CFD can't completely reproduce a complicated field. On the other hand measurements include some errors involving their method. Therefore measured data can't completely satisfy the governing equations and can't cover the whole of a target region because of its difficulty. In order to understand accurate flow and scalar fields, it is necessary to correct measured data so that the governing equations are satisfied as much as possible and to complement the region without measured data by the governing equations. In this study, a cost function (Shiota 2000) which consists of the remainders of the governing equation and the difference between observed values and the solutions was proposed. This method was applied for a two-dimensional room and the performances of the cost function method were examined.

## COST FUNCTION

We defined the cost function (CF) as the sum of the square of two terms that represent the remainders of the governing equation such as the Navier-Stokes

**Akira Kondo, Hiroshi Nakagawa, Akikazu Kaga and Yoshio Inoue are** in the Engineering for Assessing the Sustainable Engineering, Graduate School of Engineering, Osaka University.

equation, the continuity equation and the conservative equations of scalars, and the difference between observed values and the solutions. We introduce an equivalent coefficient for evaluating each term equivalently, an accuracy coefficient based on the accuracy of the observed values, and a weighting coefficient that weights each term according to the purpose of analysis. The cost function is expressed by

$$CF = \int \left\{ \sum_k \alpha_k \beta_k f_k{}^2 \left( \xi_i, \eta_j \right) + \sum_j \alpha_j \beta_j C_j \left( \eta_j - \eta_{j,obs} \right)^2 \right\} d\xi \qquad (1)$$

where $\xi$ is the independent variable, $\eta$ is the dependent variable, $f$ is the governing equation. $\alpha$ , $\beta$ , and $C$ are a weighting coefficient, an equivalent coefficient, and an accuracy coefficient, respectively. $\eta_{,obs}$ is the observed value. The meaning of each subscript is summarized in Table 1.

**Table 1. The meaning of each subscript**

| | $i$ | $j$ | $k$ |
|---|---|---|---|
| 1 | coordinate of $x$ direction | wind component of $x$ direction ($u$) | N-S equation of $u$ component |
| 2 | coordinate of $y$ direction | wind component of $y$ direction ($v$) | N-S equation of $v$ component |
| 3 | coordinate of $z$ direction | wind component of $z$ direction ($w$) | N-S equation of $w$ component |
| 4 | time | Pressure ($p$) | continuity equation |
| 5 | | Temperature ($T$) | conservative equations of temperature |
| 6 | | Concentration ($c$) | conservative equations of concentration |

The equivalent coefficients are chosen so that each term of the cost function may become equal, when each independent variable changes to the surroundings of the solution by the uncertainty of the same order. However, as the solution is generally unknown, we use the CFD results as an alternative value and vary the values at each point randomly with the maximum errors estimated by assuming the use of typical measurement instruments and measurement techniques. In this study, both a weighting coefficient and an accuracy coefficient are assumed to be a constant of a unity.

The optimum solution is obtained by minimizing the cost function and is expressed by

$$\int \left\{ \sum_k \alpha_k \beta_k f_k \frac{\partial \left( f_k \right)}{\partial \eta_j} + \alpha_j \beta_j C_j \left( \eta_j - \eta_{j,obs} \right) \right\} d\xi = 0 \qquad (2)$$

The combination of $\partial \left( f_k \right) / \partial \eta_j$ in the second term of the equation (2) is shown in Table 2. In order to optimize wind component, the Navier-Stokes equation and the continuity equation are partially differentiated with respect to wind component

like $\partial f_1/\partial u, \partial f_2/\partial v, \partial f_3/\partial w$ and $\partial f_4/\partial u, \partial f_4/\partial v, \partial f_4/\partial w$ . Similarly in order to optimize temperature $T$, the conservative equation of temperature are partially differentiated with respect to temperature $T$ like $\partial f_5/\partial T$ . We call the solution of these types the individual type solution. The conservative equations of temperature and concentration are the function of wind components so that they may be optimized by partially differentiated with respect to wind components $u,v.w$ like $\partial f_5/\partial u, \partial f_5/\partial v, \partial f_5/\partial w$ and $\partial f_6/\partial u, \partial f_6/\partial v, \partial f_6/\partial w$ . Similarly the Navier-Stokes equation of wind component $w$ (Boussinesq approximate) is the function of temperature so that it may be optimized by partially differentiated with respect to temperature $T$ like $\partial f_3/\partial T$ . We call the solution of these types the intergraded type solution.

**Table 2. The combination of $\partial f_k/\partial \eta_j$**

| $\eta_j$ \ $f_k$ | 1 | 2 | 3 | 4 | 5 | 6 |
|---|---|---|---|---|---|---|
| $u$ | 0 | (0*) | (0*) | 0 | 0* | 0* |
| $v$ | (0*) | 0 | (0*) | 0 | 0* | 0* |
| $w$ | (0*) | (0*) | 0 | 0 | 0* | 0* |
| $p$ | 0 | 0 | 0 | | | |
| $T$ | | | (0*) | | 0 | |
| $c$ | | | | | | 0 |

* represents the intergraded type solution. Theoretically (0*) represents the integrated type solution but isn't used in this study.

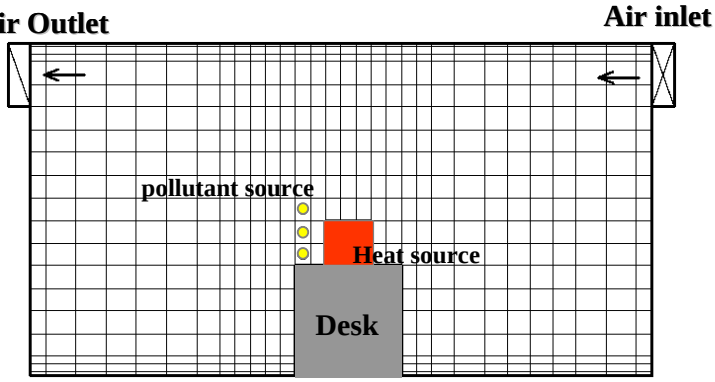


***Figure 1*** *Objective room*

## APPLICATION FOR CF

### Objective room

The objective region is a two dimensional room as shown in Figure 1. The obstacle is set in the center of this room. Heat source and pollutant source is set above this obstacle. The size of this room is 4000mm (W) X 2200mm (H).The both sizes of inlet and outlet are 425mm.

**Table 3. Boundary conditions**

| | |
|---|---|
| Inlet | **20cm/s** uniformly |
| Outlet | free boundary |
| Heat source | 200W : **Heat flux at the top is 4 times larger than at the latera**l. |
| Pollutant source | Ratio of emission flux is **1:2:3** from bottom mesh. |
| Wall | Adiabatic condition |

### Observed value

The observed value can't be measured because of the imaginary room. CFD calculation was carried out according to the boundary conditions as shown in Table 3 and the calculated results were used as the alternative values of observed values.

These observed values of wind field, temperature, and concentration are shown in Figure 2.

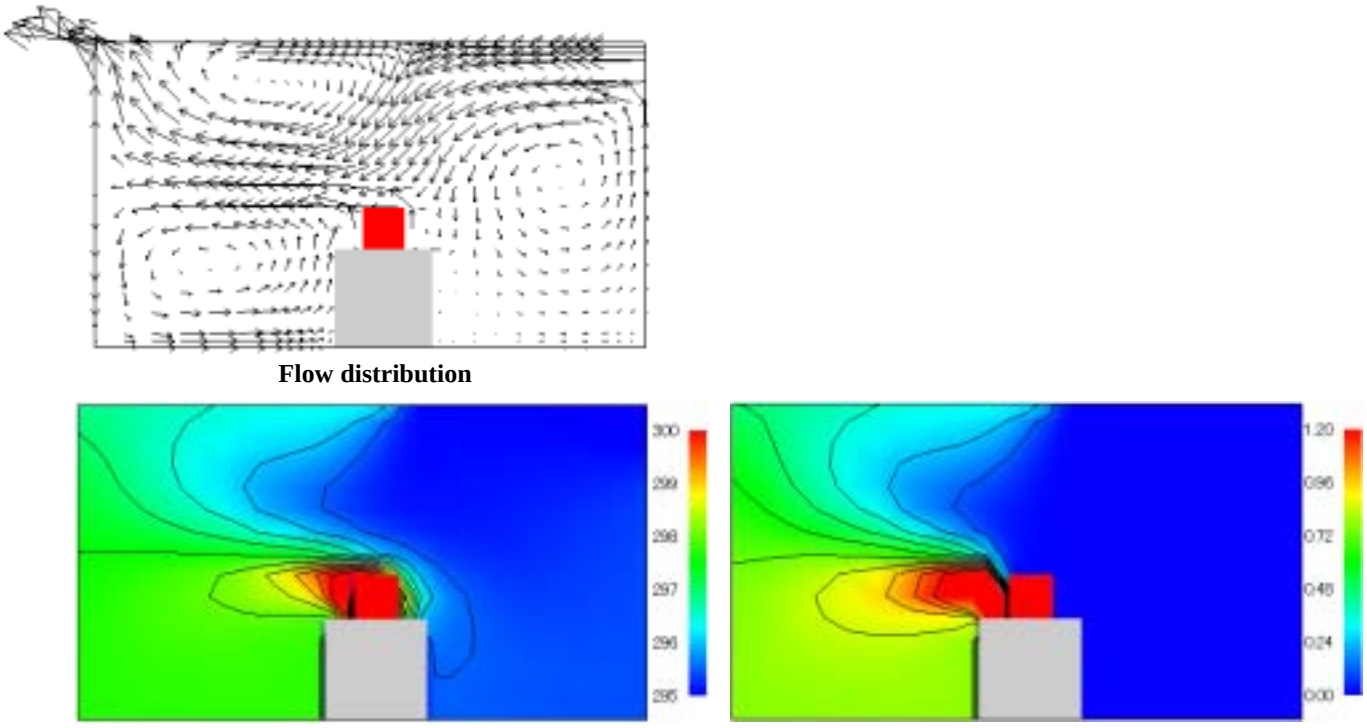


***Figure 2*** *Observed values*

**CFD results**

If the boundary conditions of the objective region are obvious, the CFD results become almost same as the observed values in Figure 2. However, the boundary conditions of the actual room are not perfectly obvious. Therefore CFD calculation must be carried out by using the uncertain boundary conditions and the CFD results are somewhat different from the observed values. The CFD calculation by using the incorrect boundary conditions compared with Table 2 was assumed to be the CFD results. The incorrect boundary conditions are shown in Table 4. These CFD results of temperature, concentration and wind field are shown in Figure 3. In Figure 3, the downward wind occurred at the neighborhood of inlet. In Figure 2, the downward wind occurred above the obstacle. The region with high temperature existed above the obstacle in Figure 2, and existed at the left-bottom of the obstacle in Figure 3. The region with high concentration can see in the left-bottom in Figure 3 compared with Figure 2.

Using the Statistical indexes of root mean square error ( $RMS$) (Equation (3)) and mean absolutely error ( $MEA$ ) (Equation (4)), both indexes between the observed values and the CFD results were evaluated and was summarized in Table 5.

**Table 4. Incorrect boundary conditions**

| | |
|---|---|
| Inlet | **16cm/s** uniformly |
| Outlet | free boundary |
| Heat source | 200W : **Heat flux at the top is the same as the lateral.** |
| Pollutant source | Ratio of emission flux is **1:1:1** from bottom mesh. |
| Wall | Adiabatic condition |

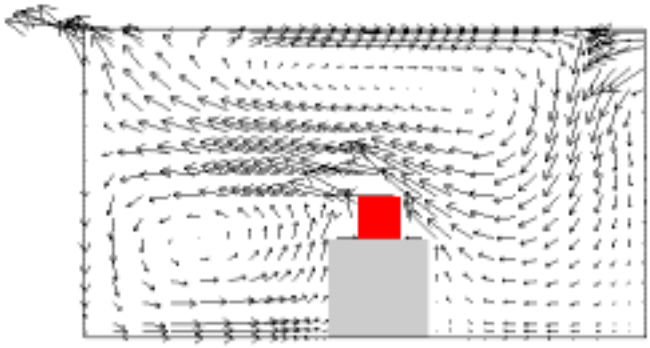

**Flow distribution**

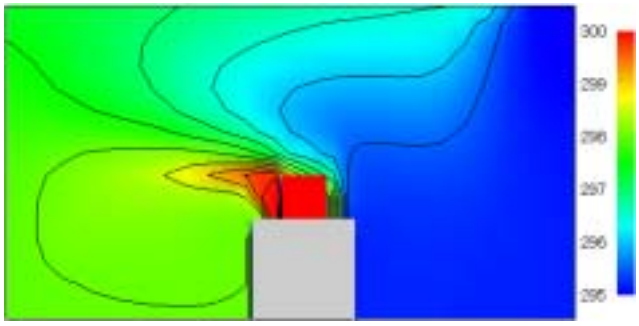


**Temperature distribution**

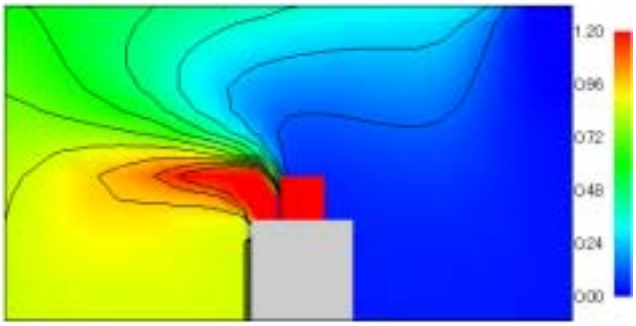


**Concentration distribution**

***Figure 3*** *CFD results*

$$RMS(\eta_j) = \sqrt{\frac{\sum_N (\eta_{j,obs} - \eta_j)^2}{N}} \quad (3)$$

$$MAE(\eta_j) = \frac{\sum_N \left|\eta_{j,obs} - \eta_j\right|}{N} \quad (4)$$

**Table 5. error between observed values and CFD results**

| $RMS(u)$ | $MAE(u)$ | $RMS(v)$ | $MAE(v)$ | $RMS(T)$ | $MAE(T)$ | $RMS(c)$ | $MAE(c)$ |
|---|---|---|---|---|---|---|---|
| 0.0576 | 0.0332 | 0.0410 | 0.0264 | 0.565 | 0.448 | 0.135 | 0.107 |

## PERFORMANCE OF CF

The CFD results calculated by using the incorrect boundary conditions were corrected by combining the observed values according to the equation (2). As the correct boundary conditions weren't obvious, the governing equations in the equation (2) were solved by using the incorrect boundary conditions.

### Individual type solution

**Flow field.** The flow fields of the CFD results were corrected by using the observed data of three regions as shown in Figure 4; (a)windward of inlet, (b) above of the obstacle, and (c) the left-bottom. The flow fields corrected by each data are shown in Figure 5. In the cases of (a) and (b), the large vortex in the right side of this room was revised. If the small region crossing the main current was corrected by observed data, the flow field in the whole of this room was trend to be corrected. In the case of (c), the flow field was locally revised but the flow field in the whole of this room wasn't revised. The performances defined by the equation (5) and (6) were evaluated and were summarized in Table 6. The performances were improved in all cases and the high improvement was seen in the cases (a) and (b).

$$P(\eta)_{RMS} = \frac{RMS_{obs-CFD} - RMS_{obs-revised}}{RMS_{obs-CFD}} \times 100 \qquad (5)$$

$$P(\eta)_{MAE} = \frac{MAE_{obs-CFD} - MAE_{obs-revised}}{MAE_{obs-CFD}} \times 100 \qquad (6)$$

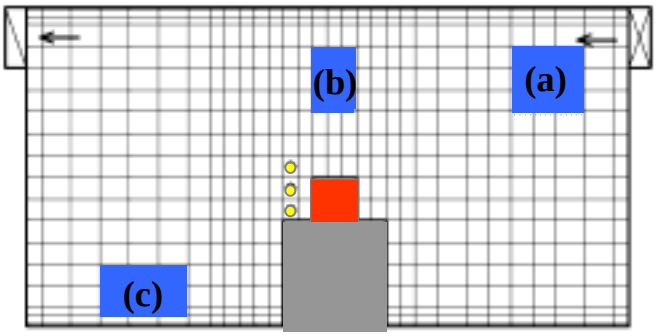


***Figure 4*** *Regions of observed velocity*

**Table 6. Performance of CF (%)**

| | (a) | (b) | (c) |
|---|---|---|---|
| $P(u)_{RMS}$ | 72 | 65 | 60 |
| $P(u)_{MAE}$ | 51 | 52 | 51 |
| $P(v)_{RMS}$ | 51 | 57 | 27 |
| $P(v)_{MAE}$ | 44 | 52 | 27 |

**Temperature field.** The temperature fields of the CFD results were corrected by using the observed data of two regions as shown in Figure 6; (a) above the obstacle and (b) close to the outlet. The temperature fields corrected by each data are shown in Figure 7. In both cases, the dispersion of high temperature in the left bottom of this room was suppressed compared with the CFD results. The performances were summarized in Table 7. The fourth columns in Table 7 showed the case revised by both observed data. Obviously the use of both data improved the performances than the use of one data.

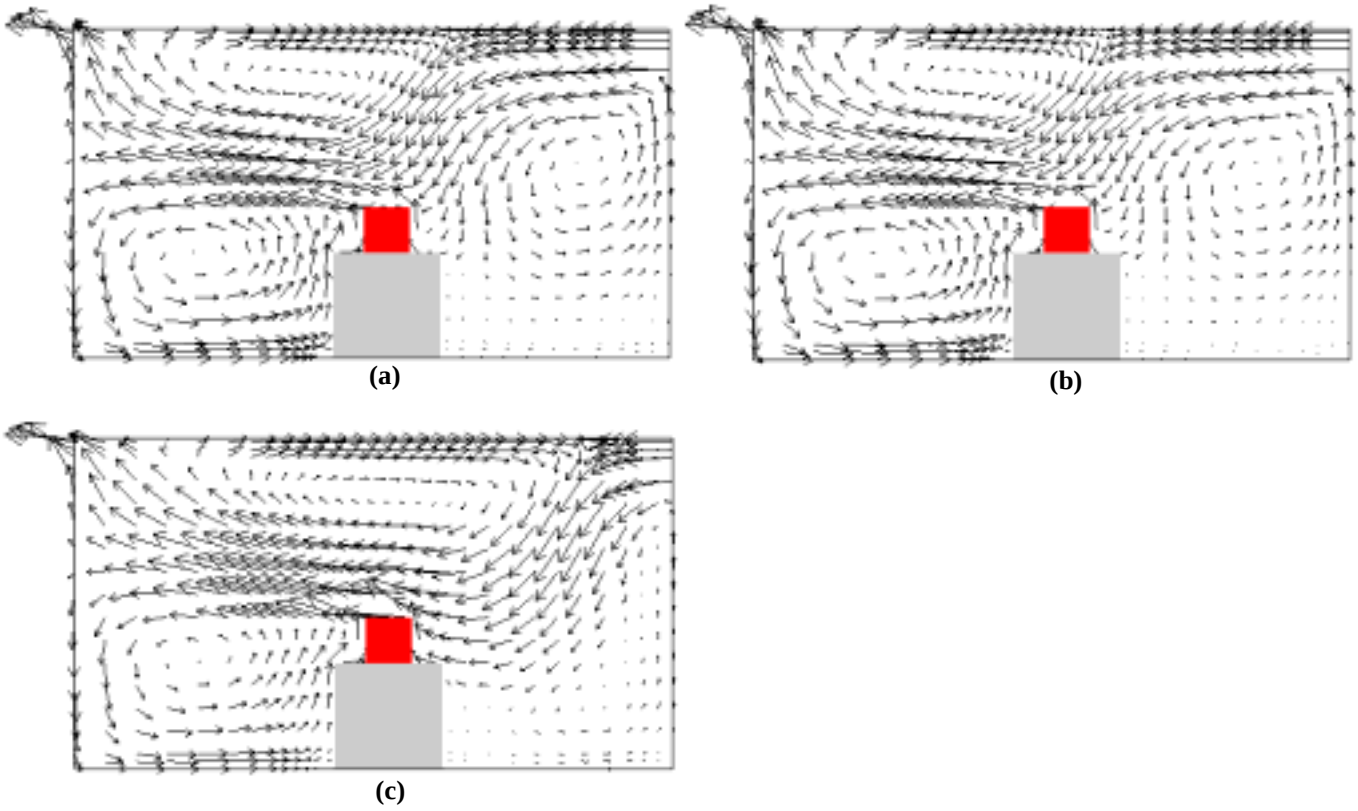


***Figure 5*** *Corrected flow fields*

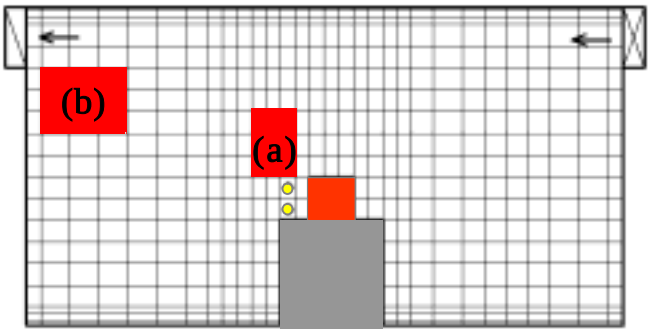


***Figure 6*** *Regions of Observed temperature*

**Table 7. Performance of CF (%)**

| | (a) | (b) | (a)+(b) |
|---|---|---|---|
| $P(T)_{RMS}$ | 38 | 38 | 63 |
| $P(T)_{MAE}$ | 35 | 38 | 69 |

**Concentration field.** The concentration fields of the CFD results were corrected by using the observed data of two regions as shown in Figure 8; (a) above the obstacle and (b) close to the outlet. The concentration fields corrected by each data are shown in Figure 9. In the case of (a), the region of high concentration appeared at the left side of the obstacle compared with the observed data. In the case of (b), the region of high concentration at the left side of the obstacle disappeared but the concentration level generally become low compared with the observed data. The performances were summarized in Table 8. The fourth columns in Table 8 showed the case revised by both observed data. These values were almost

same as the values in the case of (a). This means that the region (a) was dominant to determine the concentration fields of the whole of this room.

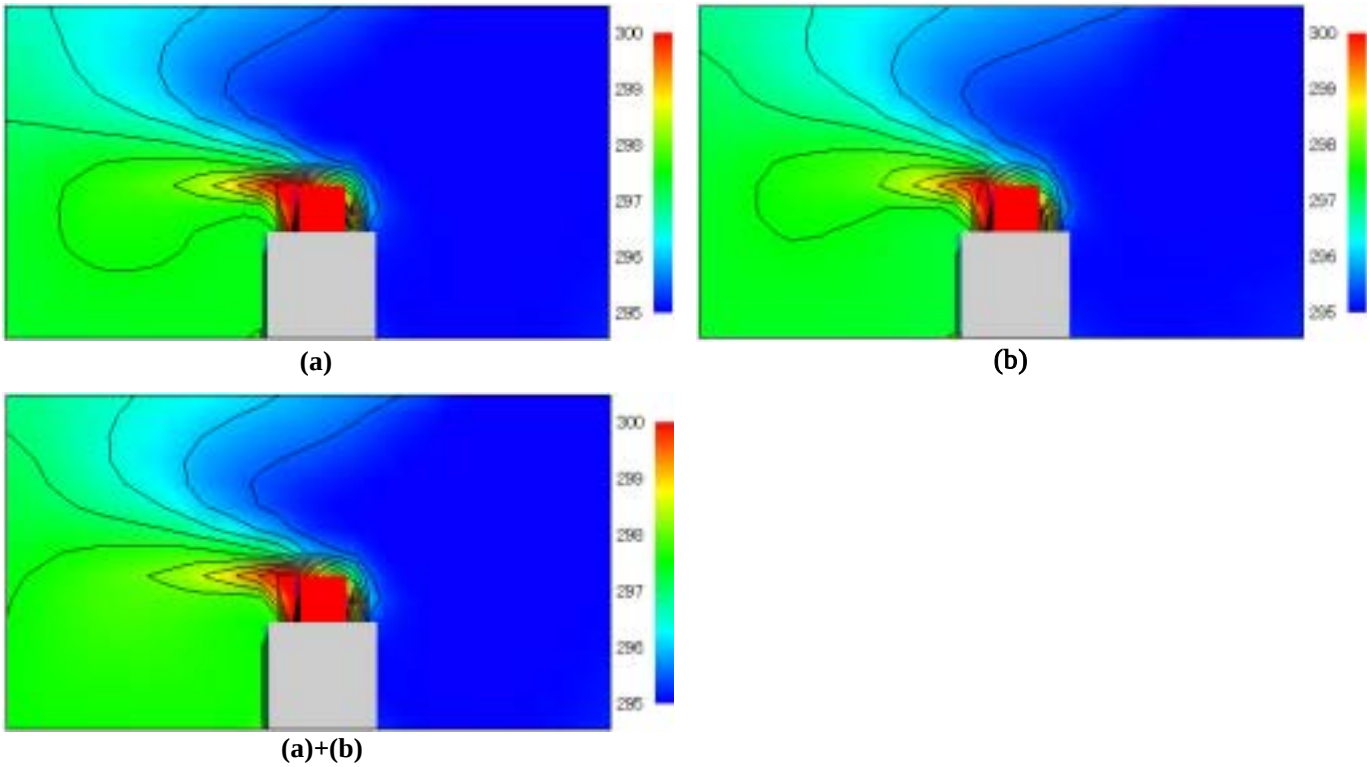


***Figure 7*** *Corrected temperature fields*

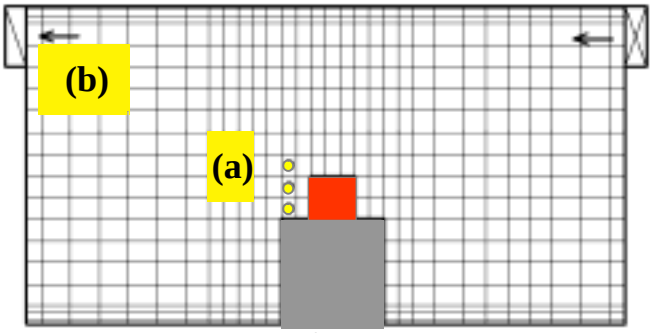


***Figure 8*** *Regions of Observed concentration*

**Table 8. Performance of CF (%)**

| | (a) | (b) | (a)+(b) |
|---|---|---|---|
| $P(c)_{RMS}$ | 41 | 15 | 46 |
| $P(c)_{MAE}$ | 29 | 15 | 41 |

**Integrated type solution**

The flow fields of the CFD results were corrected by using (a) the temperature data and (b) the concentration data as shown in Figure 10. The flow fields corrected by each data are shown in Figure 11. In the cases of (a) and (b), the large vortex in the right side of this room was revised. The improvement was naturally small compared with Figure 5(a) and 5(b) that was revised by directly the wind speed data but was large compared with Figure 5(c). The performances were

summarized in Table 9. The fourth columns in Table 9 showed the case revised by both data. Obviously the use of both data improved the performances than the use of one data.

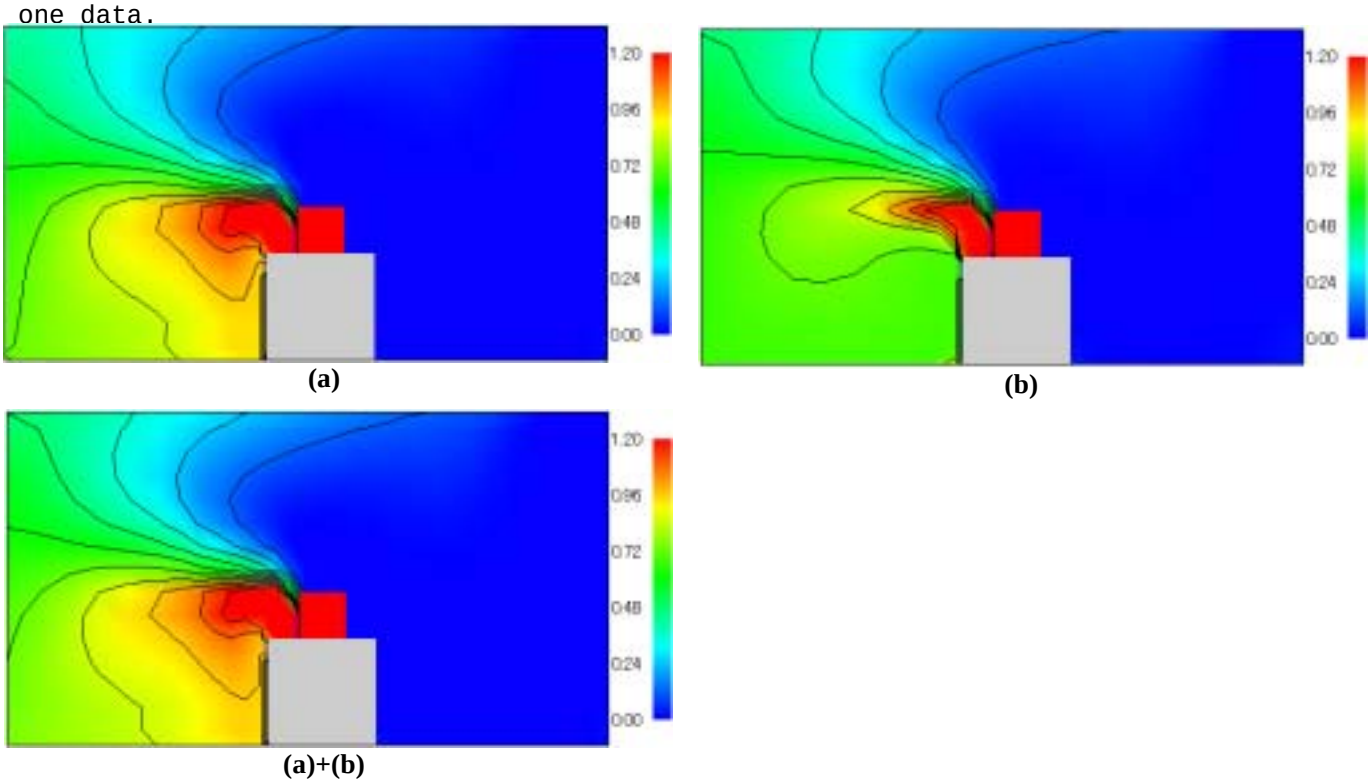


***Figure 9*** *Corrected temperature fields*

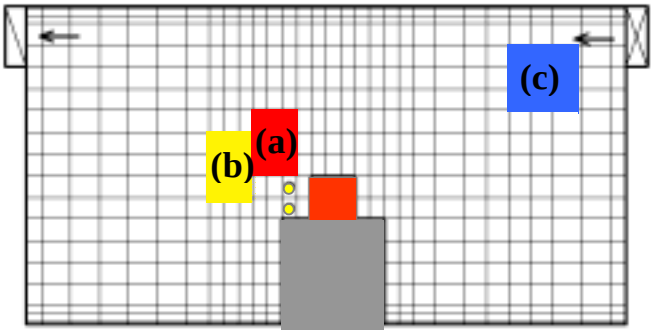


***Figure 10*** *Regions of Observed data*

**Table 9. Performance of CF (%)**

| | (a) | (b) | (a)+(b) |
|---|---|---|---|
| $P(u)_{RMS}$ | 64 | 69 | 68 |
| $P(u)_{MAE}$ | 58 | 61 | 63 |
| $P(v)_{RMS}$ | 39 | 45 | 60 |
| $P(v)_{MAE}$ | 30 | 43 | 58 |

**Comparison individual type solution with integrated type solution**

The CFD results were corrected by using the three observed data as shown in Figure 10; (a) temperature, (b) concentration, and (c) wind field. The performances of both the individual type solution and the integrate type solution were compared and were summarized in Table 10. The performances of the integrated type solute for all variables were considerably better than the performances of the individual type solution. These high performances were showed by repeating that the flow fields

revised by the scalar data revised the scalar data.

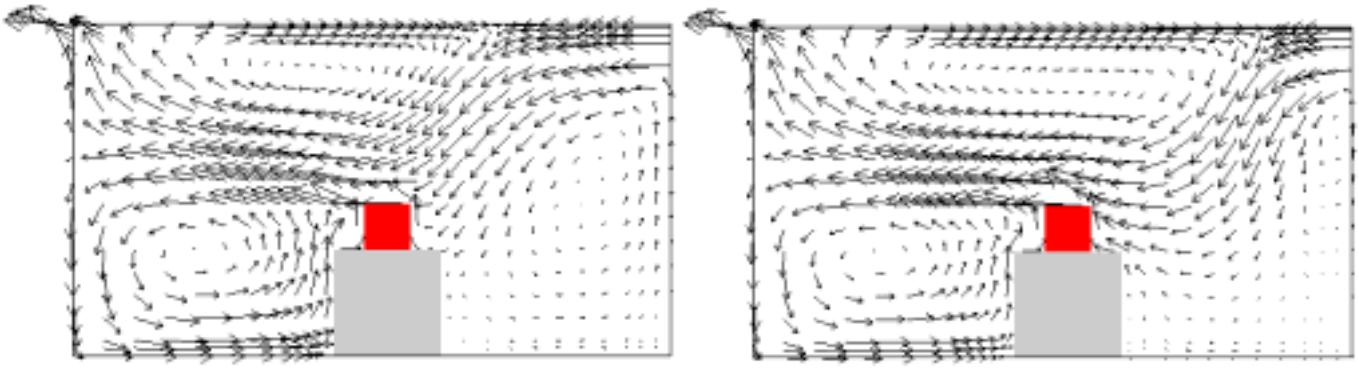

**(a)** **(b)**

***Figure 11*** *Corrected flow flieds*

**Table10. Performance of CF (%)**

| $P(u)_{RMS}$ | $P(u)_{MAE}$ | $P(v)_{RMS}$ | $P(v)_{MAE}$ | $P(T)_{RMS}$ | $P(T)_{MAE}$ | $P(c)_{RMS}$ | $P(c)_{MAE}$ |
|---|---|---|---|---|---|---|---|
| 56 | 25 | 30 | 26 | 8 | 4 | 4 | -22[1] |
| 73 | 72 | 76 | 75 | 51 | 53 | 67 | 53 |

The top presents the performance of the individual type solution and the bottom presents the performance of the integrated type solution.

## CONCLUSION

A cost function expressed by the remainders of the governing equations and the difference between observed values and the solutions was proposed in this study. This method was applied for a two-dimensional room and the performances of the cost function method of *RMS* and *MEA* were examined. In the individual type solution (which the governing equation of a variable is partially differentiated with respect to itself) the performances of the flow fields, the temperature field, and the concentration fields were improved by combining the observed data. The performances were varied by the region of observed data. In the integrated type solution (which the governing equation of a variable is partially differentiated with respect to another variable) the performances of the flow fields were remarkably improved by combining the temperature data or the concentration data. The performances were varied by the region of observed data. The performances of the integrated type solution for combining three data of temperature, concentration and wind components gave the excellent results for all variables than that of the individual type solution.

## REFERENCES


Kaga, A., Inoue, Y. and Yamaguchi, Y. 1993. Pattern tracking algorithm using successive abandonment. J. Flow Visualization, 1: 283-296

Laundar, B.E., Reece, G.J. and Rodi, W. 1975. Progresses in the development of a Reynolds-stress turbulent closure. J. Fluid Mech., 68: 537-566

Leonard, A. 1974. Energy cascade in large eddy simulation of turbulent fluid flow. Advances in Geophysics, 18A, 237-248.

Rodi, W. 1976. A new algebraic relation for calculating the Reynolds stress. ZAMM, 56: 219-221
Shiota, T., Yamaguchi, K., Kaga, A., Kondo, A. and Inoue, Y. 2000. Combined Technique of PIV and CFD Using Cost Function and Comparison with FDDA. 9th Int. Symp. on Flow Visualization, 205

 